momentum, and so flow in radially. Such purely radial 'Bondi–Hoyle' flows have very low radiation efficiencies. Melia then showed that a 10^{-4}-solar-mass yr^{-1} Bondi–Hoyle flow onto a million-solar-mass black hole would produce something like the observed radio to X-ray spectrum of SgrA*, including its weak infrared emission[4]. However, even small deviations from the purely radial flow would create a very large amount of infrared radiation, inconsistent with the observations; and such deviations would be likely to occur, at least transiently, through incomplete mixing of the incoming wind gas, or interactions with a pre-existing fossil accretion disk.

The new work of Narayan *et al.*[1] follows a second route. In a hot accretion flow, the gas is ionized to form a plasma. The heavy ions carry most of the mass, and thus of the energy, whereas the electrons produce most of the radiation (through synchrotron, Compton and Bremsstrahlung radiation processes). But, crucially, in a low-density flow the temperatures of the ions and of the electrons may decouple[8–10]. As a consequence, most of the gravitational energy would be viscously converted into thermal energy of the ions (in a hot ion torus[9,10]), and not radiated away by the electrons.

Instead, the gravitational energy is carried ('advected') with the flow across the event horizon of the black hole[11,12]. Such a flow leads to a low radiation efficiency even in a highly dissipative accretion disk. The possible application of such a model to the Galactic Centre had already been proposed more than a decade ago[13], but Narayan *et al.* have now shown that a quantitative and self-consistent dynamical model can be constructed that fits most of the SgrA* observations for a 2.6-million-solar-mass black hole accreting at 10^{-4} solar masses per year. Like Melia's Bondi–Hoyle model, this advection-dominated accretion flow model also explains the spectral shape of the observed emission, with peaks in the millimetre and X-ray bands but very weak emission in the near-infrared and visible.

Turning the argument around, Narayan *et al.* point out that the success of their model (and the Melia model) leaves little doubt that the dark mass in the Galactic Centre must indeed be a black hole in the strict sense of General Relativity. Only if an event horizon exists can the gravitational energy truly disappear from sight. Otherwise there would have to be a 'surface' where the gravitational and thermal energy of the flow was converted to radiation after all. This argument adds to the already strong case for the existence of black holes.

Naturally, there remain some uncertainties. First, one might question how well the current accretion rate is determined by the observations. Apart from an order-of-magnitude uncertainty in the accretion rate estimated above, time variability in the flow may be important. However, the dynamical time for the stellar winds near SgrA* is only about 100 years, and high-energy X-ray observations indicate that SgrA* was not very much more active 100 years ago than it is now. (Hard X-rays are scattered by dense, interstellar clouds. By looking at that scattered radiation from clouds about 100 light years from SgrA*, one can thus infer its X-ray brightness 100 years ago.) Second, the detailed plasma physics of the advection flow and the reality of the two-temperature solution are complex matters that depend on a number of poorly known parameters.

Nevertheless, the new work is the best answer yet to this strange paradox. Why are many massive black holes so black? It is because most of the time they are converting their food very inefficiently into radiation. □

Reinhard Genzel is at the Max-Planck Institut für Extraterrestrische Physik, W-8046 Garching, Germany.
e-mail: genzel@mpe.mpg.de

1. Narayan, R., Mahadevan, R., Grindlay, J. E., Popham, R. G. & Gammie, C. *Astrophys. J.* **492,** 554–568 (1998).
2. Kormendy, J. & Richstone, D. *Annu. Rev. Astron. Astrophys.* **33,** 581–624 (1995).
3. Miyoshi, M. *et al. Nature* **373,** 127–129 (1995).
4. Genzel, R., Eckart, A., Ott, T. & Eisenhauer, F. *Mon. Not. R. Astron. Soc.* **291,** 219–234 (1997).
5. Falcke, H., Biermann, P. L., Duschl, W. J. & Mezger, P. G. *Astron. Astrophys.* **270,** 102–106 (1993).
6. Melia, F. *Astrophys. J.* **387,** L25–L28 (1992).
7. Ozernoy, L. in *Back to the Galaxy* (eds Holt, S. S. *et al.*) 40–43 (AIP, New York, 1992).
8. Ichimaru, S. *Astrophys. J.* **214,** 840–855 (1977).
9. Shapiro, S. L., Lightman, A. P. & Eardley, D. M. *Astrophys. J.* **204,** 187–199 (1976).
10. Rees, M. J., Begelman, M. C., Blandford, R. D. & Phinney, E. S. *Nature* **295,** 17–21 (1982).
11. Begelman, M. C. *Mon. Not. R. Astron. Soc.* **184,** 53–67 (1978).
12. Abramowicz, M., Czerny, B., Lasota, J. P. & Szuskiewicz, E. *Astrophys. J.* **332,** 646–658 (1988).
13. Rees, M. in *The Galactic Center* (eds Riegler, G. R. & Blandford, R. D.) *Am. Inst. Phys. Conf. Proc.* **83,** 166–176 (1982).

Neurobiology

The analytical bend of the leech

L. F. Abbott

Descartes introduced the coordinate system that forms the basis of analytical geometry in an appendix to a philosophical discourse[1] that has been criticized for its contemptuous tone[2]. Descartes might have been more humble had he known that his great discovery had already been implemented in the nervous systems of invertebrates, and that it is used by the leech to direct a reflexive motor behaviour. The evidence provided by Lewis and Kristan on page 76 of this issue[3] arrives too late for Descartes, but in time to show the rest of us how a network of neurons computes a sensory–motor transformation.

Leeches respond to a touch on their skin by bending away from the point of contact. In each body segment, four sensory neurons (the P neurons) represent the location of the touch stimulus. They generate the response by activating a set of motor neurons through a network of interneurons. Lewis and Kristan have now determined the touch locations that evoke the maximum activity from each of the P neurons. Relative to the dorsal midline, these are at angles of 45, 135, 225 and 315 degrees, thereby forming two perpendicular axes (P_1 to P_4 in Fig. 1). When a touch is made at an angle θ, lying between the preferred angles of two P neurons, they respond by firing action potentials at rates proportional to $\cos(\theta)$ and $\sin(\theta)$, while the other two P neurons remain silent. Cosine and sine projections onto perpendicular coordinate axes are the defining features of a cartesian coordinate system. For any touch location, the firing rates of two active P neurons serve as cartesian coordinates. Four neurons are required to cover all directions because firing rates cannot represent negative coordinate values. Here the leech is in good company — Descartes was also reluctant to use negative coordinates, and it was left to Newton to point out their usefulness[2].

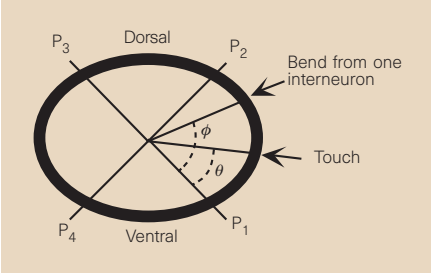

Figure 1 **Computation of a sensory–motor transformation by neurons in the leech. The shaded area represents a cross-section of the body wall of the leech. Four sensory neurons (P cells) fire maximally in response to touches of the skin at the directions denoted by the lines P_1, P_2, P_3 and P_4. Lewis and Kristan[3] have found that touches at other locations evoke responses in pairs of P cells at rates proportional to the cosine and sine of the angle θ defining the location of the touch. Also shown is the angle ϕ defining the bend produced by activation of a single interneuron.**

As every student of introductory physics will testify, it is one thing to set up a cartesian coordinate system and quite another to use it computationally. Lewis and Kristan provide convincing evidence that the leech bending network takes full advantage of the cartesian representation it has established. They show that the touch location inferred by interpreting P-neuron fire rates as cartesian coordinates accurately matches the actual stimulus

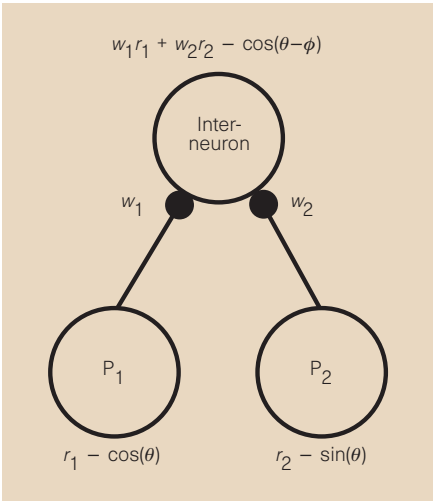

Figure 2 **A simple circuit showing two P cells driving an interneuron. The synaptic drive to the interneuron is the sum of the synaptic weights w_1 and w_2 multiplied by the corresponding P-cell firing rates r_1 and r_2. This drive is proportional to the cosine of the angle between the location of the touch and the bend produced by the interneuron.**

location (3 per cent r.m.s. error). When they injected current into a P cell to modify its activity, the change in the bending response matched the shift in the coordinate value represented by the P cell's activity. Finally, they modelled how the sensory–motor transformation[4,5] that directs the bend is computed.

The P cells activate motor neurons through a network that is estimated to contain 25 to 30 interneurons, 17 of which have been identified[6]. In the model, activation of an individual interneuron generates a bend in a particular direction characteristic of that neuron (the angle ϕ in Fig. 1). For an arbitrary touch location, different interneurons must be activated at appropriate levels so that they collectively produce the desired bend. A reasonable measure of the 'appropriate level of activation' is the projection of the desired bend direction onto the bend direction produced by the interneuron. If an interneuron generates a bend about the fixed angle ϕ when activated alone, this projection is proportional to $\cos(\theta-\phi)$. How does the bending circuitry compute this cosine?

Figure 2 shows the basic circuit element used in Lewis and Kristan's model. Two P cells drive an interneuron through synapses with strengths that are characterized by weights w_1 and w_2 (for simplicity the two inactive P cells are not shown). The total synaptic drive — given by the sum of the P-cell rates multiplied by the corresponding synaptic weights — is proportional to $w_1\cos(\theta) + w_2\sin(\theta)$. Any reader who dredges up the angle-addition law for cosines will realize that the desired quantity, $\cos(\theta-\phi)$, can be computed simply by making the synaptic weights w_1 and w_2 proportional to $\cos(\phi)$ and $\sin(\phi)$. Lewis and Kristan found that the strengths of the synaptic connections from P cells to interneurons are, indeed, proportional to the appropriate cosines and sines for all 17 identified interneurons. Futhermore, a network model constructed on this principle duplicates the performance of the leech when at least 14 interneurons are included.

This is not the first time that a cartesian representation has been seen in an invertebrate sensory system. Miller, Jacobs and Theunissen[7] found a virtually identical arrangement of four interneurons in the cricket cercal system, which responds to air currents. Neural firing rates that follow a cosine law have also been seen in a number of vertebrate systems, including the motor cortex of the monkey[8], although not in an arrangement corresponding to a cartesian coordinate system. But until now we have not had a chance to see a nervous system making use of such a representation to do actual computations.

Although the full circuitry of the bending network of the leech has not been worked out, it seems likely that one of its basic operating principles has been revealed. The P-cell/interneuron circuit is constructed to compute projections of various motor force vectors along a desired bend direction — and it performs this computation as elegantly as Descartes would have. □

L. F. Abbott is at the Volen Center and Department of Biology, Brandeis University, Waltham, Massachusetts 02254, USA.
e-mail: abbott@volen.brandeis.edu

1. Descartes, R. *La Géométrie* (Hermann, Paris, 1927).
2. Coolidge, J. L. *A History of Geometrical Methods* (Oxford Univ. Press, 1940).
3. Lewis, J. E. & Kristan, W. B. Jr *Nature* **391,** 76–79 (1998).
4. Salinas, E. & Abbott, L. F. *J. Neurosci.* **15,** 6461–6474 (1995).
5. Kristan, W. B. Jr, Lockery, S. R. & Lewis, J. E. *J. Neurobiol.* **27,** 380–389 (1995).
6. Lockery, S. R. & Kristan, W. B. Jr *J. Neurosci.* **10,** 1816–1829 (1990).
7. Miller, J. P., Jacobs, G. A. & Theunissen, F. E. *J. Neurophysiol.* **66,** 1680–1689 (1991).
8. Georgopoulos, A. P., Schwartz, A. B. & Kettner, R. E. *Science* **233,** 1416–1419 (1986).

Nanotechnology

New tricks with nanotubes

M. S. Dresselhaus

Carbon nanotubes are seamlessly rolled single sheets of carbon atoms, only a few nanometres across. Two papers in this issue, Wildöer *et al.*[1] on page 59 and Odom *et al.*[2] on page 62, present strong experimental evidence for the remarkable electronic properties that were predicted[3] in 1992 — namely, that they can be either metallic or semiconducting depending on their diameter and helicity. Both teams used scanning tunnelling microscope (STM) probes at low temperature to test these predictions, by measuring electronic structure (in terms of the density of states) and physical structure (the nanotube diameter and helicity). The results, obtained on nanotubes prepared differently and with different diameter distributions, are complementary.

The diameter and helicity of a nanotube are uniquely determined by the chiral vector (n,m), where n and m are integers (Fig. 1). For example, a (10,0) nanotube simply has ten carbon hexagons around its diameter, and no helicity — this type is called a 'zigzag' tube, as a broken end perpendicular to the axis would have a zigzag shape. To go once around a (10,10) nanotube (a type of 'armchair'), one must move ten hexagons in one direction, turn 60° and move ten more; the helicity is 30°. Theory predicts that when $n - m$ is divisible by three, the single-walled carbon nanotubes are metallic; otherwise they are semiconducting. To verify this prediction, it is necessary to measure both the electronic properties and structure of individual nanotubes.

Although nanotube structures, resolved on the atomic level by STM, have already been reported[3,4], the present papers collectively do a more systematic study. But more importantly, they relate the electronic properties of these nanotubes to their structure, primarily in terms of the one-dimensional (1D) density of electronic states along the tube axis. This is given by the derivative of the current–voltage curve, dI/dV, obtained by operating the probe as a scanning tunnelling spectroscope (STS).

Theoretical predictions for the 1D density of electronic states (Fig. 2, overleaf) of both semiconducting (10,0) and metallic (9,0) nanotubes show a series of spikes. Each spike corresponds to the energy threshold for an electronic sub-band caused by the quantum confinement of electrons in the radial and circumferential directions of the nanotubes (which are one carbon atom thick and only

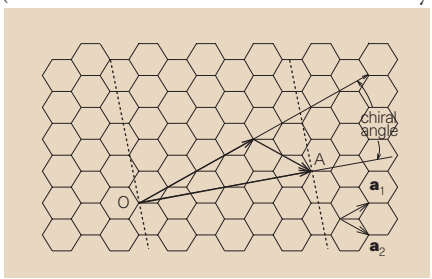

Figure 1 **Nanotube coordinates. The vector OA defines a (4, 2) nanotube which, when laid out flat, would have edges along the dotted lines. To go around the tube once and get back to one's starting point, one moves four hexagons in the $\vec{a}_1$ direction and two hexagons in the $\vec{a}_2$ direction, 60° apart.**